Proceedings of the 2004 IEEE
International Conference on Robotics & Automation
New Orleans, LA • April 2004

# A computational technique for interactive needle insertions in 3D nonlinear material

Han-Wen Nienhuys and A. Frank van der Stappen

Institute of Information and Computing Sciences
Utrecht University
PO Box 80089
3508 TB Utrecht
The Netherlands
{hanwen,frankst}@cs.uu.nl

*Abstract*— **We present a computational method for simulating needle insertions interactively in *both* 2D and 3D models of soft tissue. The approach is based on the Finite Element Method (FEM) and uses quasi-static stick-slip friction for needle/tissue interactions. The FEM equations are solved using an iterative method, and the mesh is refined adaptively near the needle trajectory. The boundary formed by the needle surface is not represented explicitly in the mesh, but its geometry is accounted for in the friction forces. This has the advantage that we can use a simple and therefore fast refinement scheme that is guaranteed to keep the mesh quality at the initial level. This approach can also be applied to the 3D situation as well as to nonlinear geometry and material models. We present results of computational experiments of the 2D simulation, and show promising samples of the 3D implementation.**

## I. Introduction

Real-time simulations of surgical procedures have the potential to offer a cheap method to train medical personnel in performing certain procedures. Simulation of needle insertions is a suitable first candidate application. The mechanics of needle insertion are relatively straightforward, making a simulation feasible. Performing accurate insertions can be difficult, making a simulation desirable: when inserting needles deeply into soft-tissue, the tissue deforms, making a target hard to reach. For example, brachytherapy treatment of prostate cancer (delivering radioactive seeds directly into the tumor with a needle) is complicated by the soft tissue surrounding the prostate. This easily leads to placement errors. When the seed is misplaced, healthy tissue instead of cancerous cells will be damaged [1]. DiMaio and Salcudean [5] list other applications, where misplacing needles can lead to complications. In summary, it seems advantageous to simulate needle insertions.

In simulating medical procedures for training purposes, realism is cited as the most important problem to solve. This poses a problem: the mechanics of living tissue are infinitely complex in the context of real-time applications: living tissue is non-compressible and anisotropic, has a non-linear strain-rate dependent stress-strain relation, and is relatively soft, which leads to large deformations and geometrically non-linear problems. Measuring tissue properties is far from trivial [6]. As an example, Székely et al. [13] have estimated that a full-scale endoscopic hysteroscopy simulation using a non-linear, dynamic and incompressible model would require a sustained performance of 20 GFLOP per second. Such performance is out of reach of current workstations, and requires a parallel processing architecture, which was only demonstrated on scaled down models.

Working from real tissue towards a simulation leads to a complex model with massive computational requirements, and many parameters which are hard to estimate. Such a simulation would be realistic on theoretical grounds. However, when we do not presuppose an unlimited amount of computational power, then it can never be close to realistic: normal workstations do not have enough power to run such a simulation quickly enough to be real-time and keep up with user input. In light of this observation, we have chosen to reverse the problem, and start with a not entirely realistic but proven approach, the one proposed by DiMaio and Salcudean [3], and improve the computational technique used in specific areas.

DiMaio and Salcudean [3–5] have presented an interactive simulation of needle insertions in a planar environment. They simulate inserting a needle into a flat slab of material. During the simulation, the elastic response of the entire slab is computed using a linear finite element model (FEM). As a result, the effects of needle flection and movements perpendicular to the insertion direction can be simulated too. This is an improvement over traditional simulators, which only simulate friction forces parallel to the needle [2]. DiMaio and Salcudean validate their model by comparing it to measurements of needle insertions made in a slab of soft plastic. Their simulation reaches haptic refresh rates on a Pentium 3/450Mhz. They achieve this by eliminating unused variables in an expensive pre-processing step; this procedure is called *condensation*. The simulation of the system is *static*: time or velocity are not modeled. Stick/slip friction models the interaction between needle and tissue in a manner consistent with the static model. In this model, friction forces only depend on the magnitude of elastic forces, and not on velocities.

We propose to improve their work to address the following shortcoming: the condensation technique cannot be extended to 3D; condensation is a precomputation technique, requiring

$\mathcal{O}(n^3)$ flops for a FEM mesh of $n$ nodes. In 3D, this becomes prohibitively expensive. In 3D, forces are applied to surfaces. Therefore, the needle (which applies friction forces to the tissue) must be represented in the mesh as a curved 3D surface. To represent this surface adequately, the mesh must include elements that are as small as the needle itself. A simple computation shows that a uniform mesh—necessary for condensation— with elements of size 1mm for a 100 mm × 100 mm × 100 mm object leads to a stiffness matrix with roughly $3 \cdot 10^6$ degrees of freedom. Condensation of internal nodes requires storing the inverse of the stiffness matrix, which is dense and occupies approximately 67 terabytes of memory.

We propose a computational technique based on *iterative algorithms*. Such algorithms do not require precomputed structures, implying that the mesh may be changed at run-time. In particular, the mesh can be *refined adaptively* in the region of interest, thus ensuring that the discretization is accurate while computational requirements remain low. Moreover, iterative algorithms can also handle models with *geometric or material nonlinearities*. These are necessary to accurately predict the results of large deformations. [11]. Incorporating arbitrary boundaries, such as the needle surface, while maintaining high mesh quality can be difficult, especially in 3D [12]. However, in our case there is no special reason to represent that boundary exactly. Instead, the geometry of the needle surface is accounted for in the magnitude of the friction forces. The advantage of this *non-conforming* approach is that no complex meshing techniques are necessary, and we can use a simple subdivision scheme that exactly maintains element shapes of the starting mesh. This ensures that the refined mesh has a *high quality*, and leads to an accurate discretization.

The rest of the paper shows how an iterative algorithm, adaptive meshing and non-conforming method are combined to produce a simulation that achieves high precision at low computational costs, and also generalizes to 3D nonlinear simulations. We demonstrate the technique in a 2D simulation that is functionally equivalent to the one shown by DiMaio and Salcudean. We also show some samples from our proof-of-concept 3D simulation.

With our method, it is possible to exchange computation time and accuracy. Computational experiments indicate that in 2D this method runs at haptic update rates on a Pentium3/1 Ghz for displacement accuracies of approximately 1 mm.

## II. Physical Model

The needle insertion is simulated by having the needle apply forces to a slab of material, and simulating the resulting deformation of the slab. This requires addressing

- the continuum mechanics of the tissue, and
- the model for friction between tissue and needle.

### A. Tissue mechanics

The 2D insertion is assumed to happen in a flat slab of elastic material (See Figure 1). In this scenario, the $z$-planes of the slab are unloaded, so we can assume that stresses in the $z$ coordinate vanish. This leads to *plane stress* [14]. By setting $z$-stresses to nil, we reduce the 3D description to 2D. For linear material, stress (The 2D second Piola-Kirchoff stress tensor $\tilde{\mathbf{S}}$) and local deformation ($\tilde{\mathbf{C}}$ is the right Cauchy-green strain tensor) are related through

$$\mu(\tilde{\mathbf{C}} - \tilde{\mathbf{I}}) + \frac{2\mu\lambda}{\lambda + 2\mu} \operatorname{trace}(\tilde{\mathbf{C}} - \tilde{\mathbf{I}})\tilde{\mathbf{I}}, \tag{1}$$

where $\lambda$ and $\mu$ are the Lamé parameters. The strain tensor $\tilde{C}$ is defined by

$$\tilde{\mathbf{C}} = (\tilde{\mathbf{I}} + \frac{\partial \mathbf{u}}{\partial \mathbf{z}})^* \cdot (\tilde{\mathbf{I}} + \frac{\partial \mathbf{u}}{\partial \mathbf{z}}) \approx \tilde{\mathbf{I}} + (\frac{\partial \mathbf{u}}{\partial \mathbf{z}})^* + \frac{\partial \mathbf{u}}{\partial \mathbf{z}}.$$

The last approximation is the linear geometry approximation, which only holds for small deformations. The identity tensor is denoted by $\tilde{\mathbf{I}}$, and $\mathbf{u}(\mathbf{z})$ is the displacement field.

For nonlinear materials, the same procedure may be used to derive 2D constitutive equations, but leads to unpalatable equations. However, when compressible neo-Hookean material [14] is presumed not to conserve volume at all (i.e., $\lambda = 0$), then has it has following stress-strain relation for the plane stress case,

$$\tilde{\mathbf{S}} = \mu(\tilde{\mathbf{I}} - \tilde{\mathbf{C}}^{-1}). \tag{2}$$

For small deformations, this reduces to the linear model in Equation 1. The assumption $\lambda = 0$ is not realistic in the context of tissue simulation, however, it allows us to quantify the errors caused by the linear elasticity assumption.

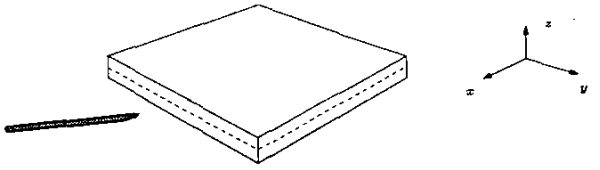


Fig. 1. Plane stress. When loading thin slabs of material, the $z$ sides are unloaded.

### B. Stick/slip friction

We assume a quasi-static loading: in this model, time is not explicitly present; instead, the slab is always in equilibrium with the externally applied loads. Without a notion of time, there is also no velocity. This forces us to model the interaction between the needle and the tissue as *stick-slip* friction. When the needle moves a small amount, material sticks to the needle. As the needle moves more, the tissue deforms, and reacts with increasing elastic force. When the elastic forces locally exceed a friction threshold, the material starts slipping across the needle. From a theoretical viewpoint, the needle forms a part of the boundary where either displacements (stick friction) or tractions (slip friction) are prescribed.

The needle is modeled as a line segment without any thickness. The effect of cutting is accounted for in the profile of the friction forces, which is inspired by DiMaio and Salcudean's work, and is shown in Figure 2. In reality, the needle cuts tissue, distending material points. Consequently, the simulation has an inherent inaccuracy: it can never be more accurate than the thickness of the needle being modeled.

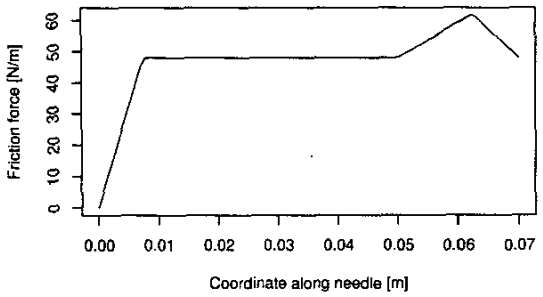


Fig. 2. Friction force varies along the shaft of the needle, and this graph shows how. The bulge at the tip accounts for force required to cut tissue.

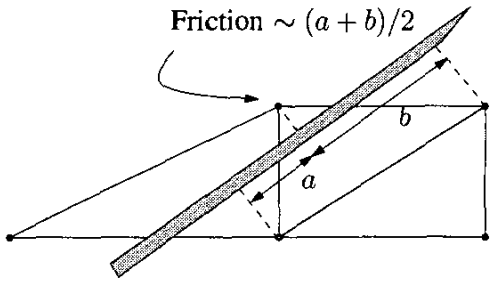


Fig. 3. Accounting for the needle/mesh geometry interaction through the forces. In 2D, nodal friction forces are proportional to the distance parallel to the needle.

## III. Computational techniques

The implementation uses the Finite Element Method as a discretization method. The resulting equations are numerically solved with an iterative solution method. As this method is matrix-free, online mesh-changes are possible. To improve accuracy, we refine the mesh near the simulated needle.

### A. Adaptive mesh refinement

We discretize the elasticity problem using the Finite Element Method (FEM) [14] on a triangle mesh. The accuracy of a FEM discretization is mainly determined by the mesh element quality and mesh density density. Hence, in a discretization of a needle insertion, we should refine the mesh near the region of interest (i.e. the needle tip), and prevent any skinny triangles from occurring. This is achieved by use of edge *edge bisection*: a triangle is refined by splitting the longest edge. By recursively splitting neighboring triangles in the same manner, mesh compatibility is maintained. This scheme is easy to implement, fast, and maintains element quality. It is illustrated in Figure 5.

### B. Needle representation

The adaptive refinement scheme does not include the exact shape of the needle as a boundary in the mesh, but we can account for this geometry in the magnitude of the friction force thresholds. The needle is represented by a set of *needle nodes* that are close to the needle. The friction thresholds for these nodes are determined by their distance parallel to the needle. More precisely, from every mesh edge intersected by the needle, the closest node is considered to be a needle node. For the sequence of needle nodes, the distance components parallel to the needle shaft are computed; see Figure 3. These distances are used with the force distribution in Figure 2 to compute friction thresholds.

Needle nodes have two states: either a node is fixed (sticking), which means that its location is attached to the user controlled needle, or its movement is constrained to be parallel to the needle shaft (slipping). A configuration of slipping and sticking nodes leads to a single static deformation problem. When the solution of this problem is found, the elastic reaction forces can be used to rearrange the boundary conditions. Needle nodes whose elastic force exceeds the friction threshold are marked as slipping, and the others are marked as sticking. Both sticking and slipping needle nodes are constrained so they cannot move perpendicular to the needle.

### C. Generalizing to 3D

This scheme can be extended to 3D insertions. Edge bisection generalizes to tetrahedral meshes [7] (also illustrated in Figure 5). In 3D, the friction force is proportional to the area where it acts. For computing the frictions, an internal surface is selected, and the resulting friction is proportional to the area of the needle shaft that it covers. The shaft is considered to be a cylinder. Tetrahedra inside and close to the needle shaft form *needle tetrahedra*. The boundary of this set is an internal surface of the mesh, and each triangle of this surface has a friction threshold, which is distributed over its incident nodes. This contribution is computed by projecting the triangle onto the cylindrical shaft, and multiplying the projected area with a friction density derived from Figure 2.

### D. Relaxation

We use the nonlinear Conjugate Gradient (CG) method [10] for solving elasticity equations. This is an optimization method that finds the configuration with minimal potential energy. The method is as efficient as dynamic relaxation using lumped masses [9], but has no stability problems. The CG method can be applied to both linear and nonlinear elasticity, and can cope with changing boundary conditions. It can be implemented using a matrix-free setting, so there is no need to store precomputed structures. The method decreases potential energy until the following stopping criterion is achieved

$$\|f^{\text{extern}} + f^{\text{elastic}}\|_2 < \varepsilon \sqrt{\|f^{\text{extern}}\|_2^2 + \|f^{\text{reaction}}\|_2^2}.$$

The tolerance $\varepsilon$ controls the *relaxation error*: the lower $\varepsilon$, the more accurate the numerical solution. The quantities $f^{\text{elastic}}$, $f^{\text{extern}}$ and $f^{\text{reaction}}$ are the $\mathbb{R}^{2n}$ vectors ($\mathbb{R}^{3n}$ in 3D) containing elastic forces, externally applied forces, and reaction forces

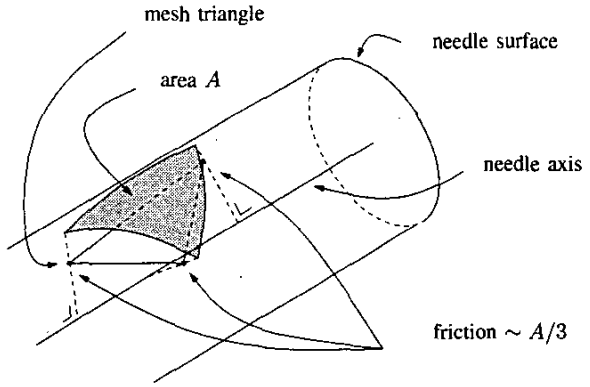


Fig. 4. Accounting for the needle/mesh geometry interaction through the forces in 3D. Friction forces normally are proportional to the surface area where they act on. In our scheme, a mesh surface close to the needle axis is selected. Triangles of this surface are projected on the surface of the needle (indicated in grey). Friction forces for triangles are proportional to the projected area.

| Average error [mm] | | | | | |
|---|---|---|---|---|---|
| $\downarrow h_{\text{start}}/h_{\text{ref}} \rightarrow$ | $h_3$ | $h_4$ | $h_5$ | $h_6$ | $h_7$ |
| $h_1$ | 0.34 | 0.33 | 0.33 | 0.30 | 0.28 |
| $h_2$ | 0.26 | 0.24 | 0.24 | 0.21 | 0.20 |
| $h_3$ | 0.15 | 0.13 | 0.13 | 0.10 | 0.08 |
| $h_4$ | | 0.09 | 0.08 | 0.04 | 0.03 |
| $h_5$ | | | 0.07 | 0.03 | 0.00 |
| $h_6$ | | | | 0.02 | 0.00 |
| Maximum error [mm] | | | | | |
| $\downarrow h_{\text{start}}/h_{\text{ref}} \rightarrow$ | $h_3$ | $h_4$ | $h_5$ | $h_6$ | $h_7$ |
| $h_1$ | 1.01 | 0.88 | 0.88 | 0.87 | 0.87 |
| $h_2$ | 0.91 | 0.68 | 0.61 | 0.54 | 0.53 |
| $h_3$ | 0.66 | 0.54 | 0.51 | 0.29 | 0.27 |
| $h_4$ | | 0.45* | 0.43 | 0.19 | 0.14 |
| $h_5$ | | | 0.41 | 0.17 | 0.06 |
| $h_6$ | | | | 0.16 | 0.03 |

TABLE I

DISPLACEMENT ERRORS FOR DIFFERENT MESH RESOLUTIONS.

(e.g., forces required to keep constrained nodes in their fixed positions) for every node.

Mesh refinements leads to new nodes and new nodal variables. Displacements are interpolated from the field. Such changes in the mesh reset the CG algorithm, which finds the new solution in an ensuing relaxation step.

## IV. COMPUTATIONAL EXPERIMENTS

First the general FEM engine was validated by subjecting it to standard cantilever beam loading tests, and comparing the computed results with theoretical solutions [9]. After this, we conducted experiments to assess whether our approach is practically feasible for needle insertion. As far as the physical model is concerned, both our scheme and the one of DiMaio and Salcudean are equivalent, since they use the same elasticity model and friction parameters. Hence, the question is: how accurate is the system for a given amount of computation?

The setting of the experiment is the test object used by DiMaio and Salcudean; it is a slab with dimensions $100 \times 100 \times 10$ mm, and material properties $E = 34\,\text{kPa}$, $\nu = 0.34$. The object is meshed as follows: first it is uniformly refined so elements have size $h_{\text{start}} = h_k = 100 \cdot 2^{-k}$ mm for some nonnegative $k$. A static load is applied corresponding to the friction resulting from a needle insertion. Around the needle, the mesh is refined so elements have sizes $h_{\text{ref}}$.

The impact of mesh resolution on the solution error was analyzed by comparing the results for $h_{\text{ref}} = h_{\text{start}} = h_7$ with results for coarser meshes. Table I lists average and maximum displacement errors in mm for element sizes varying from $h_1$ to $h_7$ compared to a solution computed at $h_{\text{ref}} = h_{\text{start}} = h_7$. Half of the table is empty, since $h_{\text{ref}} \leq h_{\text{start}}$. We see that smaller $h$ size leads to smaller errors in general. The entry marked with * roughly corresponds to mesh sizes used by Alterovitz et al. [1] and DiMaio and Salcudean [5]. We see that maximum displacement errors of approximately 0.3 mm can be attained by refining elements to size $h_6$ in the vicinity of the needle, using a starting mesh with edge lengths of $h_3$; this mesh is shown in Figure 6.

In our approach the mesh does not contain the exact needle geometry. To assess the magnitude of the error introduced by this non-conformance, we have also implemented a conforming scheme in which the nodes selected as needle nodes are projected orthogonally onto the needle. We insert a needle such that it does not coincide with the mesh edges. By comparing the difference between scenarios without and with node relocation with the solution computed at higher mesh density, we can estimate the relative effect of representing the needle exactly. These results (obtained with $h_{\text{start}} = h_3, h_{\text{ref}} = h_6$) are in Table II, and they show that the non-conformance effect is smaller than the discretization errors, thus validating our approach.

| | average error [mm] | max error [mm] |
|---|---|---|
| with relocation vs. without | 0.019 | 0.23 |
| error with relocation | 0.094 | 0.43 |
| error without relocation | 0.095 | 0.37 |

TABLE II

MAGNITUDE OF CONFORMANCE ERRORS.

The relaxation error, introduced by using the iterative CG algorithm, is relatively small. Table III shows how the value of the tolerance $\varepsilon$ in the stopping criterion in Section III affects displacement errors, by comparing solutions of the same problem calculated at different tolerances with one obtained for $\varepsilon = 10^{-8}$. This experiment has been run on a mesh with $h_{\text{ref}} = h_{\text{start}} = h_7$. Very modest tolerance values (0.1) suffice to make the errors smaller than discretization errors.

The above settings were determined using static deformation tests. These settings are used for the needle insertion simulator, which uses deformation computations to calculate the results of stick/slip friction. As the needle advances into the slab, the mesh is refined to $h_{\text{ref}}$ around the needle tip. With $h_{\text{ref}} = h_6$ and $h_{\text{start}} = h_3$, the simulation reaches an average update rate in excess of 700 Hz on a Pentium3/1Ghz. This frequency

| relaxation tolerance $\varepsilon$ | average error [mm] | maximum [mm] |
|---|---|---|
| 0.3 | 0.74 | 2.98 |
| 0.1 | 0.061 | 0.18 |
| 0.03 | 0.034 | 0.083 |
| 0.01 | 0.011 | 0.022 |
| 0.003 | 0.0038 | 0.0096 |
| 0.001 | 0.0008 | 0.0021 |

TABLE III

ERROR DEPENDENCY ON TOLERANCE.

is the number of solution stick/slip configurations computed per second. It excludes the costs of user-interaction and visualization, but includes the costs of mesh refinement and associated updates of the solution.

Our method does not exploit the linearity of the problem, so we can also use it for nonlinear material models. Figure 6 shows a scenario that involving large deformations. The needle is inserted sideways into a slab of material fixed at the bottom. The needle describes a trajectory that is curved relative to the object in its rest configuration. The material is set to have Poisson-ratio $\nu = 0$, so Equation (2) applies, and the simulation can be done both with neo-Hookean[1] and linear elasticity. The difference between the final location of the needle tip in both experiments is approximately 8 mm, which is significantly larger than all the other errors analyzed. Update rates for the nonlinear experiment are just a factor 2 lower.

The 2D system was designed with the intent of generalizing it to three dimensions. This generalization has also been implemented in a prototype, and samples are shown in Figure 7. In 3D, smaller elements are necessary to approximate the needle surface correctly. In the case of Figure 7, almost 30,000 elements were necessary, an increase of a factor 47 over the example in Figure 6. Since 3D matrix operations are also 2 to 3 times as expensive, the total computational cost of a 3D simulation is roughly a factor 120 larger.

## V. DISCUSSION

In this paper we have presented a novel method for computing deformations during simulated needle insertions into 2D and 3D elastic material. The method builds on previous work by its use of a quasi-static model of stick/slip friction with 2D plane-stress elasticity. It is different in that it uses an iterative (and optionally nonlinear) relaxation algorithm, and adaptive mesh resolution, making a generalization to 3D possible. The mesh used has a high degree of regularity, and is refined near the inserted needle to improve the local accuracy. Nodes are not moved within the mesh, so the refinement technique, edge bisection, does not cause element shape deterioration.

To assess the cost/accuracy ratio of this method, the 2D method was implemented in a prototype and subjected to computational experiments. The performance of the method is related to coarseness of the mesh, and material model used. Both factors are related to the accuracy of the end-result, so it is possible to improve response times by sacrificing accuracy. We conclude that accuracies around 1 mm for insertion in linearly elastic objects of size $100 \times 100$ mm can be achieved at haptic update rates on a 1 Ghz PC. At these rates, the discretization error (caused by coarseness of the mesh), conformance error (caused by our nonconforming scheme), relaxation error (caused by using an iterative algorithm), and rounding errors taken together are below 1 mm. These tests do not pretend to be exhaustive, but rather a demonstration that our approach is feasible. More testing would be necessary to determine in more detail to which scenarios it is applicable. For this reason, the source code of the complete simulation and the computational experiments is publicly available [8].

Given the result of our experiment with neo-Hookean elasticity (which introduced a difference of 8 mm), we see that a good tissue model is crucial to making accurate predictions of tissue deformations. Therefore, research into improvements in computational techniques should be accompanied by a more in-depth analysis of the mechanical properties of the organs being modeled.

A complete analysis should also include sensitivity to needle flexion, since we assume the needle to be rigid. Furthermore, the influence of variations in material parameters should also be investigated. Presumably, non-uniform material can be simulated by refining the mesh in areas where material parameters are highly variable.

We have conducted tests with square slabs and cubes as deformable objects. This simplifies implementation, but it is not an essential restriction: the only requirement successful for recursive edge bisection, is that vertices of the original grid are ordered [7].

Our approach generalizes to 3D. This 3D generalization has also been implemented, thus showing its feasibility. However, the computional costs of a 3D simulation are still too high for haptic applications. Iteration counts of the CG algorithm are very low in both the 2D and 3D simulation. This can be explained by the high spatial coherence between subsequent solutions and limited mesh resolution outside the region of interest. This suggests speed-ups should not be sought in techniques that decrease CG iteration counts (such as preconditioning and multigrid techniques), but in techniques that improve raw computation power: dedicated hardware and parallel processing.

[1] When this experiment was performed with the St. Venant-Kirchoff model (linear material with nonlinear geometry) this lead to inverted elements, resulting in stalling convergence

## REFERENCES


[1] R. Alterovitz, K. Goldberg, J. Pouliot, R. Taschereau, and I.-C. Hsu. Surgical needle insertion and radioactive seed implantation: Simulation and sensitivity analysis. In *IEEE International Conference Robotics and Automation (ICRA)*, 2003.

[2] P. N. Brett, T. J. Parker, A. J. Harrison, T. A. Thomas, and A. Carr. Simulation of resistance forces acting on surgical needles. *Journal of Engineering in Medicine*, 211(13):335–347, September 1997.

[3] S. P. DiMaio and S. E. Salcudean. Needle insertion modelling and simulation. In *IEEE International Conference Robotics and Automation (ICRA)*, 2002.

[4] S. P. DiMaio and S. E. Salcudean. Simulation of percutaneous procedures. In T. Dohi and R. Kikinis, editors, *Medical Image Computing and Computer Assisted Intervention (MICCAI)*, number 2489 in LNCS, pages 253–260. Springer-Verlag, 2002.

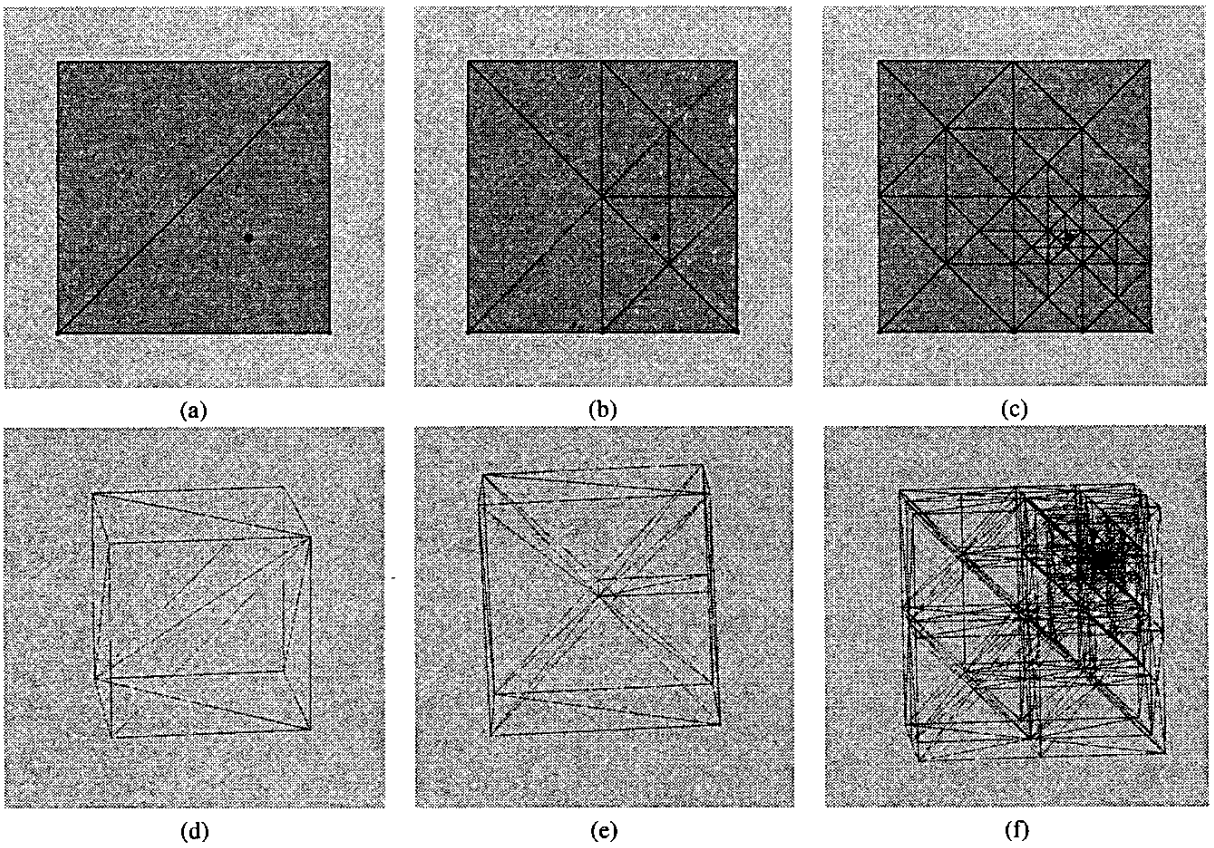


Fig. 5. Recursive edge bisection, with refinement around a single point. Picture (a) shows the starting mesh. Picture (b) and (c) shows the effect of 5 and 10 refinements. Pictures (d), (e) and (f) show 0, 3 and 20 refinements in 3D.


[5] S. P. DiMaio and S. E. Salcudean. Simulated interactive needle insertion. In *Tenth Symposium on Haptic Interfaces for Virtual Environment and Teleoperator Systems*, pages 344–351. IEEE, 2002.

[6] M. Kauer, V. Vuskovicz, J. Dual, G. Székely, and M. Bajka. Inverse finite element characterization of soft tissues with aspiration experiments. *Medical Image Analysis*, 6(3):275–287, September 2002.

[7] J. M. Maubach. Local bisection refinement for $n$-simplicial grids generated by reflection. *SIAM Journal for Scientific Computing*, 16(1):210–227, January 1995.

[8] H.-W. Nienhuys. Artisjokke—interactive needle insertions. http://www.cs.uu.nl/groups/AA/virtual/surgery/artisjokke/, 2003.

[9] H.-W. Nienhuys. *Cutting in deformable objects*. PhD thesis, Utrecht University, 2003.

[10] J. Nocedal. Theory of algorithms for unconstrained optimization. *Acta Numerica*, 1:199–242, 1992.

[11] G. Picinbono, H. Delingette, and N. Ayache. Non-Linear Anisotropic Elasticity for Real-Time Surgery Simulation. *Graphical Models*, 2002. In press.

[12] J. R. Shewchuk. A condition guaranteeing the existence of higher-dimensional constrained Delaunay triangulations. In *Annual ACM Symposium on Computational Geometry*, pages 76–85. Association for Computing Machinery, 1998.

[13] G. Székely, Ch. Brechbühler, R. Hutter, A. Rhomberg, N. Ironmonger, and P. Schmid. Modelling of soft tissue deformation for laparoscopic surgery simulation. *Medical Image Analysis*, 4(1):57–66, March 2000.

[14] O. C. Zienkiewicz and R. L. Taylor. *The Finite Element Method*, volume 1 and 2. Butterworth-Heinemann, 2000.

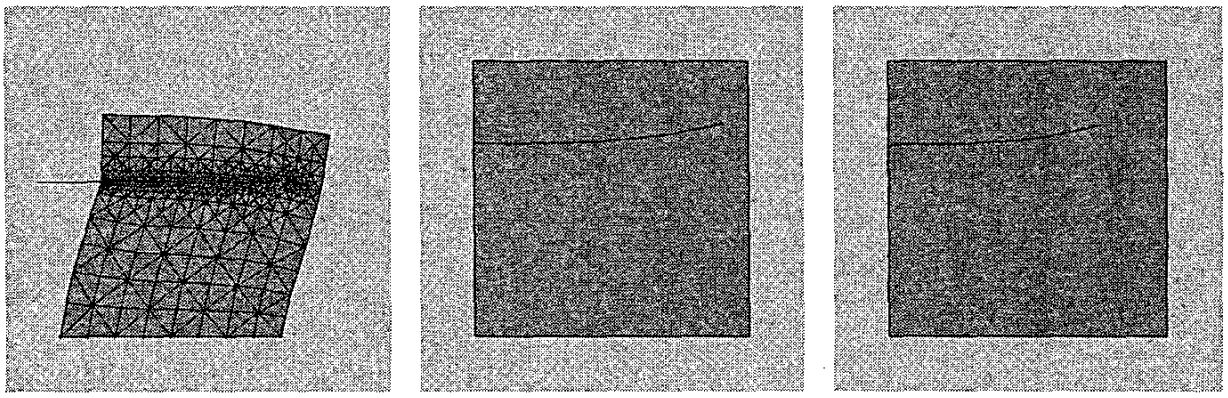


Fig. 6. Neo-Hookean (left and center) linearly elastic material (right) compared. A needle insertion sideways into slab of elastic material (10 cm × 10 cm) Poisson ratio $\nu = 0$) fixed on the bottom was simulated for two material models. The left picture shows the deformed configuration for neo-Hookean material, the center and right picture the reference configurations for neo-Hookean and linear material. The distance between the tip location in both reference locations in both experiments is approximately 8 mm. The simulation for the nonlinear case took approximately 38 seconds on a P3/1Ghz and ended with a mesh of 625 elements.

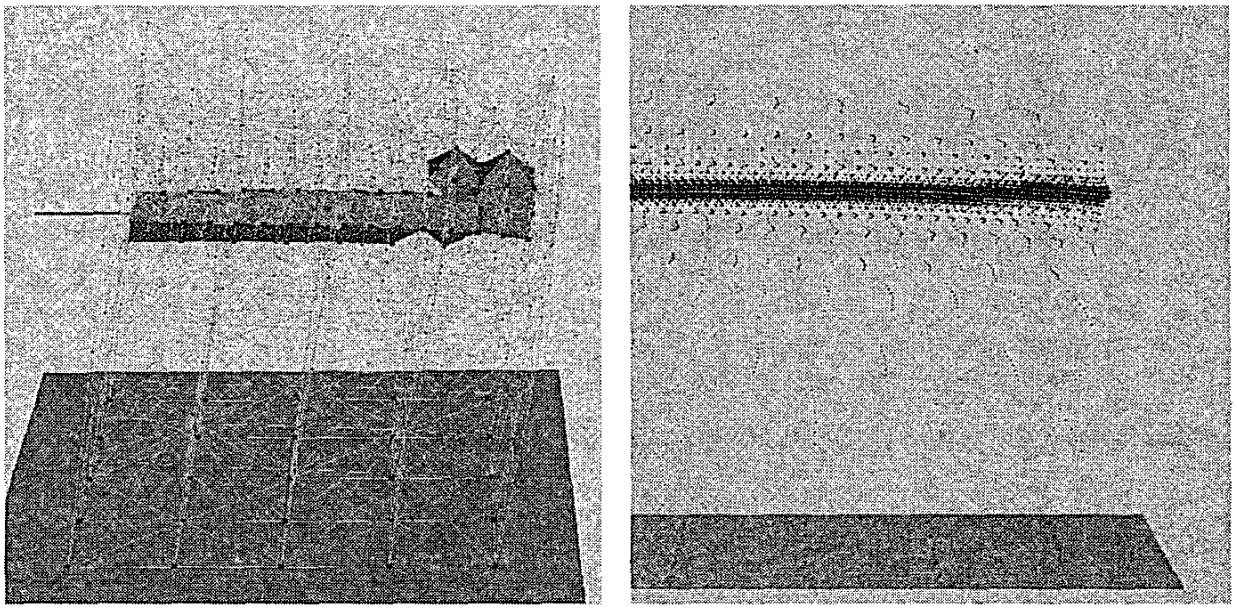


Fig. 7. Insertions of a needle (radius 1 mm) from the left into a elastic cube (10 cm × 10 cm × 10 cm) fixed on the bottom. The needle surface is drawn solid; the surface is jagged, but the result remains valid due to how forces are chosen. Left: linear material, 12 fold refinement around the needle. On the right a detail from a similar insertion into neo-Hookean material, with 20 fold refinement around the needle (Mesh edges are not shown). Timings were done on a P3/1Ghz. The needle exits the object in the right picture, but doesn't in the left one, showing that material model and mesh resolution can affect the outcome of a simulation.